Research on Dynamic Modeling Method of Single Linkage Flexible Robotic Arm

Xingquan Gao [1], Hao Guo [2], Xu Chen [2], Yang Sun [2], Decai Xu [2] and Dongdong Huang [2]

[1]Jilin Institute of Chemical Technology Jilin Vocational College of Industry and Technology, Jilin, China

[2]Jilin Institute of Chemical Technology, Jilin, China

Abstract. In this paper, a dynamics modeling method is proposed for a single-link flexible robotic arm. Firstly, the dynamic equation of the flexible manipulator system is deduced by using the Lagrange equation, secondly, the nonlinear model of the single-link flexible robotic arm is obtained by separating the spatio-temporal variables using the assumed modes method, and the model is verified by the Quanser flexible robotic arm experimental platform. Finally, the model is modified for the dead zone of the actuator found in the experimental process, which improves the accuracy of the model.

Keywords: single-link flexible robotic arm; assumed modes method; Lagrange equation.

1. Introduction

Compared with rigid robotic arm, flexible robotic arm composed of flexible structures have larger working space and higher safety performance, but at the same time, their flexible and lightweight characteristics are also more susceptible to buffeting caused by external influences, which deepens the Due to the complexity of the system, establishing an accurate mathematical model is the premise of in-depth research and wide application of flexible robotic arm.

For single-linked flexible robotic arm, the widely used modeling methods include Newton-Euler method, Kane equation, Lagrange method, etc. [1]. The dynamic equation derived by the Newton-Euler method, in which the internal force term appears can clearly express the complete force relationship of the system. G Ferretti et al. [2] used the Newton-Euler method to successfully calculate the mathematical model of the flexible robotic arm. However, since each step of the calculation needs to solve the objective function, it is relatively more complicated; The Kane equation uses the generalized velocity as the independent variable to describe the motion of the system, thereby deriving the dynamic equation. Ertunc et al. [3] used the Kane equation to establish a single-link flexible manipulator model. This method can eliminate the internal force term in the equation and simplify it. The role of the operation, but not intuitive enough; The Lagrange equation is suitable for systems with relatively simple structure or few degrees of freedom, and at the same time, it can avoid the internal force term in the equation, which is easy to convert to the model. Sasiadek et al. [4] used Lagrange equation to deduce the dynamic model of the double-linked flexible robotic arm.

When modeling, the deformation of the flexible connecting rod is usually described with discrete methods such as the assumed mode method, the finite element method, the transfer matrix method, and the lumped mass method. Through finite element analysis, Halim et al. [5] transformed the flexible link into a series of finite-degree-of-freedom unit aggregates to obtain the dynamic equation of the flexible robot system, and He et al. [6] proposed the concept of distributed parametric system, and used the assumed modes method to describe the elastic deformation of the double linkage flexible robot arm. The assumed modes method can separate the variables whose states are coupled with each other in a discrete manner, thereby reducing the complexity of the model operation. In this paper, the elastic deformation of the flexible link is described by the assumed modes method, and the mathematical model of the single-link flexible robotic arm is established by using the Lagrange equation.

2. Modeling

2.1 Research subjects

The single linkage flexible robot arm system produced by Quanser Canada is used as the controlled object for this study. As shown in Fig. 1, the single linkage flexible robot arm system mainly consists of three parts: servo mechanism, pressure sensor and flexible linkage.

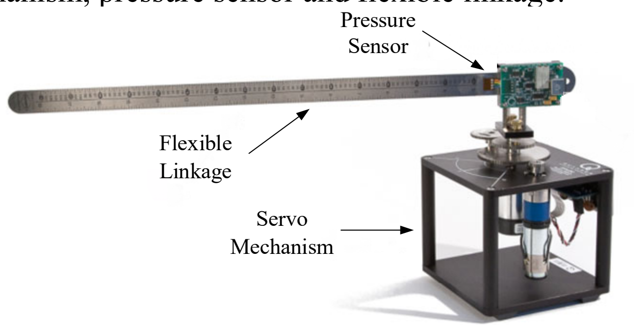

Figure 1. Single-link flexible robotic arm system.

Some of the parameters of the single-link flexible robotic arm system are shown in the table above. When working, firstly, the control signal is given by the computer, through the data acquisition card digital-to-analog conversion, then the signal is transmitted to the servo mechanism after filtering and amplifying by the power amplifier, and finally the servo motor drives the flexible linkage to rotate in the horizontal plane according to the size of the control signal.

2.2 Model building

Establish a sketch of the plane motion of the single-link flexible robot arm as shown in Fig 2 and define the inertial coordinate system in order to accurately describe the elastic vibration state of the flexible linkage SOZ with rotational reference coordinates soz. Where l denotes the length of the flexible linkage, the O point is the center of rotation of the servo mechanism, and τ represents the control torque.

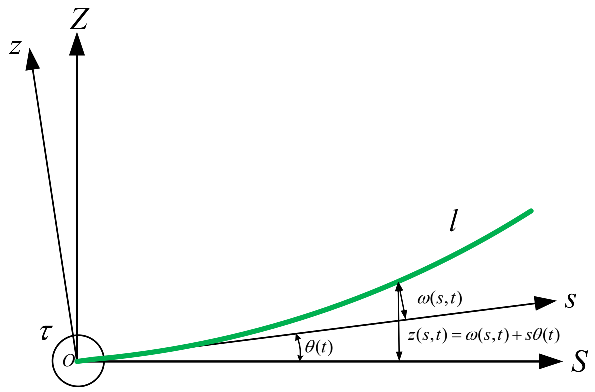

Figure 2. Simulation diagram of flexible robotic arm movement.

As a distributed parameter system, it is necessary to describe the elastic deformation of the flexible linkage in terms of time and position together. Here, $\omega(s,t)$ is used to represent the elastic vibration of the flexible link in the soz coordinate system, and $\theta(t)$ is used to represent the rotation angle of the servo mechanism. Finally, the absolute displacement of the single-link flexible manipulator in the SOZ coordinate system can be obtained as $z(s,t)=\omega(s,t)+s\theta(t)$.

According to the working principle of the system, the force that drives the rotation of the flexible linkage comes from the control torque τ which acts directly on the servo motor, i.e. $Q=\tau-Beq\dot{\theta}$, the Beq is the viscous friction coefficient of the servo system, so the Lagrange equation of the system can be obtained as

$$\begin{cases} \dfrac{\partial^2 L}{\partial t \partial \dot{\theta}} - \dfrac{\partial L}{\partial \theta} = \tau - Beq\dot{\theta} \\ \dfrac{\partial^2 L}{\partial t \partial \dot{\alpha}} - \dfrac{\partial L}{\partial \alpha} = 0 \end{cases} \tag{1}$$

Where α denotes the end vibration deflection angle of the flexible linkage, According to the physical properties of the flexible robot arm in motion, it is known that the kinetic energy of the system comes from the rotational motion, and after neglecting the effect of gravity, only the elastic potential energy generated by the elastic deformation of the flexible linkage exists. Therefore, the total kinetic energy and potential energy of the single linkage flexible arm system can be expressed as

$$\begin{cases} E_k = \dfrac{1}{2} Jeq\dot{\theta}^2 + \dfrac{1}{2}\rho\displaystyle\int_0^l \left[\dot{z}(s,t)\right]^2 ds \\ E_p = \dfrac{1}{2}\displaystyle\int_0^l EI\left[\omega''(s,t)\right]^2 ds \end{cases} \tag{2}$$

Where $\dot{z}(s,t)$ represents the partial derivative of absolute displacement with respect to time t. $\omega''(s,t)$ represents the second-order partial derivative of elastic vibration with respect to displacement s. E is the modulus of elasticity; I is the moment of inertia of the cross-section; ρ is the linear density of the flexible linkage; Jeq denotes the rotational inertia of the flexible robot arm. The Lagrange function of the system can be obtained

$$\begin{aligned} L = E_k - E_p = \frac{1}{2} Jeq\dot{\theta}^2 + \frac{1}{2}\rho\int_0^l \left[\dot{z}(s,t)\right]^2 ds \\ -\frac{1}{2}\int_0^l EI\left[\omega''(s,t)\right]^2 ds \end{aligned} \tag{3}$$

Bringing the above formula into equation (1) will eventually calculate a complex partial differential-integral equation system. At the same time, since the time and position variables in the equation system are coupled with each other, the difficulty of derivation and calculation is increased, so the equation needs to be discretized first.

The assumed modes method can discretize the continuous system through truncation processing and separate the spatiotemporal state of the coupling of the robotic arm, thereby reducing the complexity of the equation. In the following, the elastic deformation of the flexible linkage is discretized using the assumed modes method. It is known that the flexible linkage satisfies the basic conditions of Euler-Bernoulli beam, so only its bending deformation needs to be considered when the elastic deformation occurs. For the Euler-Bernoulli beam with equal cross section and equal density, its vibration equation [7] is

$$EI\frac{\partial^4 \omega(s,t)}{\partial s^4} + \rho\frac{\partial^2 \omega(s,t)}{\partial t^2} = 0 \tag{4}$$

The solution of the above equation can be expressed as

$$\omega(s,t) = \sum_{i=1}^{n} Q_i(s)\alpha_i(t) \tag{5}$$

So, the end vibration deflection angle $\alpha(t)$ of the flexible linkage is isolated by discretizing the elastic vibration of the flexible linkage. For the single link flexible robot arm, one end is fixed, and one end is free, which is consistent with the nature characteristics of a cantilever beam, so the boundary condition of the system is

$$\begin{cases} \omega(0,t)=0 \\ \dfrac{\partial\omega(0,t)}{\partial s}=0 \\ EI\dfrac{\partial^2\omega(l,t)}{\partial^2 s}=0 \\ EI\dfrac{\partial^3\omega(l,t)}{\partial^3 s}=0 \end{cases} \tag{6}$$

That is to say, at the fixed end: displacement is zero, the angle of rotation is zero; at the free end: bending moment is zero, shear force is zero, Finally, putting the above boundary conditions into the equation (4), the system inherent vibration function can be obtained [6]

$$Q_i(s)=\cosh\lambda_i s-\cos\lambda_i s+v_i(\sinh\lambda_i s-\sin\lambda_i s) \tag{7}$$

Among them

$$v_i=\frac{\sinh\lambda_i l-\sin\lambda_i l}{\cosh\lambda_i l-\cos\lambda_i l} \tag{8}$$

So, equation (3) can be converted to

$$\begin{aligned} L=&\frac{1}{2}Jeq\dot{\theta}^2+\frac{1}{2}\rho\int_0^l\left(s\dot{\theta}+\sum_{i=1}^n Q_i\dot{\alpha}_i\right)^2 ds \\ &-\frac{1}{2}\int_0^l EI\left(\sum_{i=1}^n Q_i^{"}\alpha_i\right)^2 ds \end{aligned} \tag{9}$$

After sorting, we can get

$$\begin{aligned} L=&\frac{1}{2}\left(Jeq+\frac{1}{3}\rho l^3\right)\dot{\theta}^2+\frac{1}{2}\rho\int_0^l\sum_{i=1}^n Q_i^2 ds\cdot\dot{\alpha}_i^2 \\ &+\rho\sum_{i=1}^n sQ_i ds\cdot\dot{\theta}\dot{\alpha}-\frac{1}{2}\sum_{i=1}^n EIQ_i^{"2}ds\cdot\alpha_i^2 \end{aligned} \tag{10}$$

In summary, the nonlinear model of the single-link flexible robotic arm can be obtained by putting the above formula into equation (1) as follows

$$\begin{cases} \left(Jeq+\dfrac{1}{3}\rho l^3+\rho\displaystyle\sum_{i=1}^n\int_0^l Q_i^2 ds\cdot\alpha_i^2\right)\ddot{\theta}+\displaystyle\sum_{i=1}^n\rho\int_0^l sQ_i ds \\ \cdot\ddot{\alpha}_i+2\rho\displaystyle\sum_{i=1}^n\int_0^l Q_i^2 ds\cdot\alpha_i\dot{\alpha}_i\dot{\theta}=\tau-Beq\dot{\theta} \\ \rho\displaystyle\sum_{i=1}^n\int_0^l sQ_i ds\cdot\ddot{\theta}+\rho\displaystyle\sum_{i=1}^n\int_0^l Q_i^2 ds\cdot\ddot{\alpha}_i-\rho\displaystyle\sum_{i=1}^n\int_0^l Q_i^2 ds \\ \cdot\alpha_i\ddot{\theta}^2+EI\displaystyle\sum_{i=1}^n\int_0^l Q_i^{"2}ds\cdot\alpha_i=0 \end{cases} \tag{11}$$

3. Experimental Analysis

Firstly, the open-loop system between the simulation model and the physical model is built on simulink and given the exact same input signal. Finally the accuracy of the model is verified by conducting comparison experiments on the experimental platform. The following figure shows the comparison of the experimental curves of the simulation model and the physical model under the step signal.

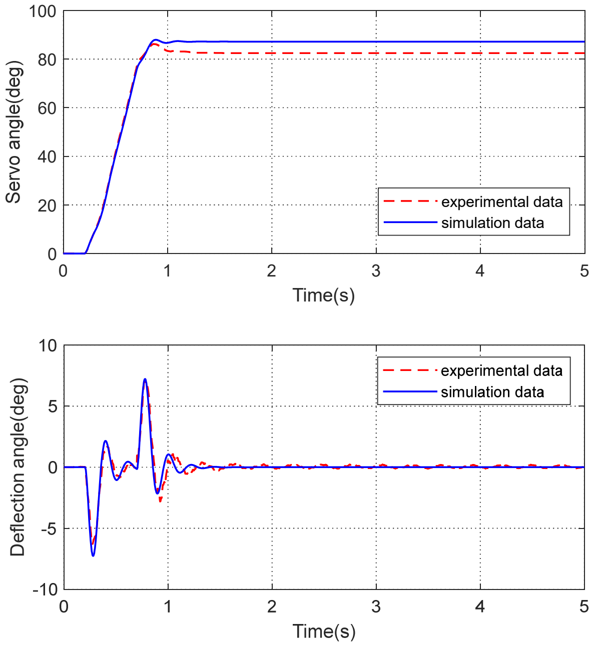

Figure 3. Simulation model and physical model comparison chart

As can be seen from the figure, the experimental results of the simulation model and the physical model are basically the same under the action of the same control signal, which proves that the flexible robotic arm model built above is correct. However, it can also be seen from the figure that the rotation angle of the final physical model is slightly smaller than that of the simulation model. Through repeated experiments, it is found that the experimental platform has no output action when the input voltage of -0.09~0.18 is given, which is considered to be caused by the median dead zone of the servo system.

In order to make the simulation model closer to the real thing, the influence of the dead zone needs to be considered here. The dead zone model of the actual output can be expressed as

$$V_{m_1}=\begin{cases} V_m-b_i, & V_m>b_i \\ 0, & b_r\le V_m\le b_i \\ V_m+b_r, & V_m<b_r \end{cases} \tag{12}$$

Among them, b_r and b_i represent the left and right range of the dead zone of the servo motor. The above open-loop experiment obtained b_r=-0.09 and b_i=0.18. Where V_m is the input voltage. Adding the dead zone to the simulation model, the control torque τ can be transformed into

$$\tau_1=\frac{\eta_g k_g \eta_m k_t\left(V_{m_1}-k_g k_m\dot{\theta}\right)}{R_m} \tag{13}$$

Where η_g is the transmission efficiency, k_g is the total transmission ratio, η_m is the motor efficiency, k_t is the motor torque constant, k_m is the counter-electromotive force constant, R_m is the motor armature resistance. After finishing, the final nonlinear mathematical model of the single-link flexible robot arm with dead zone added is obtained as follows

$$\begin{cases} \left(Jeq+\frac{1}{3}\rho l^3+\rho\sum_{i=1}^{n}\int_0^l Q_i^2 ds\cdot\alpha_i^2\right)\ddot{\theta}+\sum_{i=1}^{n}\rho\int_0^l sQ_i ds \\ \cdot\ddot{\alpha}_i+2\rho\sum_{i=1}^{n}\int_0^l Q_i^2 ds\cdot\alpha_i\dot{\alpha}_i\dot{\theta}=\tau_1-Beq\dot{\theta} \\ \rho\sum_{i=1}^{n}\int_0^l sQ_i ds\cdot\ddot{\theta}+\rho\sum_{i=1}^{n}\int_0^l Q_i^2 ds\cdot\ddot{\alpha}_i-\rho\sum_{i=1}^{n}\int_0^l Q_i^2 ds \\ \cdot\alpha_i\ddot{\theta}^2+EI\sum_{i=1}^{n}\int_0^l Q_i''^2 ds\cdot\alpha_i=0 \end{cases} \tag{14}$$

The comparison experiment is carried out again under the same conditions, and the experimental comparison curve between the simulation model with added dead zone and the physical model can be obtained as follows

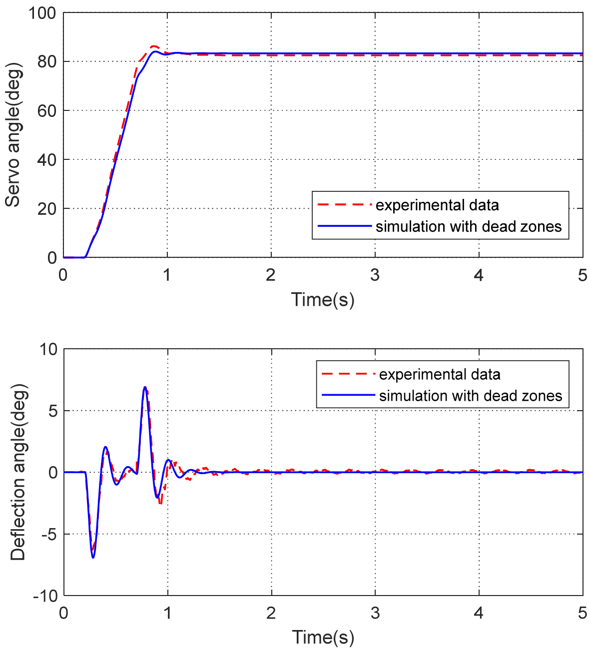

Figure 4. Add a dead-band simulation model and physical model comparison chart

As shown above, the trend of the servo angle output curves of the simulation model and the real model after adding the dead zone are basically the same, and the magnitude of the final rotation angle is also basically the same, which proves that the simulation model with the dead zone added is closer to the real one.

In the actual control design, it is necessary to decouple the above nonlinear model and linearize it, and the first-order modal function truncation process and linearization of equation (14) can be obtained

$$\begin{cases} \left(Jeq+\frac{1}{3}\rho l^3\right)\ddot{\theta}+\rho\ddot{\alpha}\int_0^l sQ_1 ds+Beq\dot{\theta}=\tau_1 \\ \rho\ddot{\theta}\int_0^l sQ_1 ds\cdot\ddot{\theta}+\rho\ddot{\alpha}\int_0^l Q_1^2 ds+EI\alpha\int_0^l Q_1''^2 ds=0 \end{cases} \tag{15}$$

Simplifying the above equation can be obtained

$$\begin{cases} M_1\ddot{\theta}+M_2\ddot{\alpha}+C_1\dot{\theta}=\tau_1 \\ M_2\ddot{\theta}+M_4\ddot{\alpha}+K_4\alpha=0 \end{cases} \tag{16}$$

Among $M_1=Jeq+\frac{1}{3}\rho l^3$, $M_2=\rho\int_0^l sQ_1 ds$, $M_4=\rho\int_0^l Q_1^2 ds$, $K_4=EI\int_0^l Q_1''^2 ds$, $C_1=Beq$.

4. Conclusions

In this paper, a nonlinear model of a single-link flexible robotic arm is established by the Lagrange equation and the hypothetical modal method, and the open-loop comparison experiment is carried out on the experimental platform, and the model is modified for the dead zone found in the experimental process, which finally proves the accuracy of the model. In addition, in view of the elastic vibration problem during the movement of the flexible robot arm, how to design the control algorithm, seek to suppress vibration and improve the control accuracy of the system needs to be further research direction in the future.

References

[1] R. K. Moolam, “Dynamic modeling and control of flexible manipu-lators,” Ph.D. dissertation, Dept. Mech. Eng., Polytech. Univ. Milan,Milan, Italy, 2014.

[2] Ferretti, Gianni, Scaglioni, et al. Closed form Newton-Euler dynamic model of flexible manipulators[J]. Robotica: International journal of information, education and research in robotics and artificial intelligence, 2017, 35(5):1006-1030.

[3] Akyuz I H , Yolacan E , Ertunc H M , et al. PID and state feedback control of a single-link flexible joint robot manipulator[C]// IEEE International Conference on Mechatronics. IEEE, 2011.

[4] Sasiadek J Z , Green A , Ulrich S , et al. Nonparametric identification and control of flexible joint robot manipulator[C]// 2014 19th International Conference on Methods and Models in Automation and Robotics, MMAR 2014. IEEE, 2014.

[5] Halim D, Xi L, Trivailo P M. Decentralized vibration control of a multi-link flexible robotic manipulator using smart piezoelectric transducers[J]. Acta Astronautica, 2014, 104(1):186-196.

[6] He W, Wang T, He X, et al. Dynamical Modeling and Boundary Vibration Control of a Rigid-Flexible Wing System[J]. IEEE/ASME Transactions on Mechatronics, 2020, PP(99):1-1.

[7] Tahmina Zebin,M. S. Alam. Modeling and Control of a Two-link Flexible Manipulator using Fuzzy Logic and Genetic Optimization Techniques[J]. Journal of Computers,2012,7(3).

[8] Sun Changyin,Gao Hejia,He Wei,Yu Yao. Fuzzy Neural Network Control of a Flexible Robotic Manipulator Using Assumed Mode Method.[J]. IEEE transactions on neural networks and learning systems,2018.